

Published in final edited form as:

*Biomacromolecules*. 2013 February 11; 14(2): 529–537. doi:10.1021/bm301785b.

## Biomimetic Polymer Brushes Containing Tethered Acetylcholine Analogs for Protein and Hippocampal Neuronal Cell Patterning

Zhaoli Zhou<sup>†,‡</sup>, Panpan Yu<sup>§</sup>, Herbert M. Geller<sup>§</sup>, and Christopher K. Ober<sup>†,‡,\*</sup>

<sup>†</sup>Department of Materials Science and Engineering, Cornell University, Ithaca, NY 14853, USA

<sup>‡</sup>Department of Chemistry and Chemical Biology, Cornell University, Ithaca, NY 14853, USA

<sup>§</sup>Developmental Neurobiology Section, Division of Intramural Research, National Heart, Lung, and Blood Institute, National Institutes of Health, Bethesda, MD 20892, USA

### Abstract

This paper describes a method to control neuronal cell adhesion and differentiation with both chemical and topographic cues by using a spatially defined polymer brush pattern. First, biomimetic methacrylate polymer brushes containing tethered neurotransmitter acetylcholine functionalities in the form of dimethylaminoethyl methacrylate (DMAEMA), or free hydroxyl-terminated poly(ethylene glycol) (PEG) units were prepared using the “grown from” method through surface-initiated atom transfer radical polymerization (SI-ATRP) reactions. The surface properties of the resulting brushes were thoroughly characterized with various techniques and hippocampal neuronal cell culture on the brush surfaces exhibit cell viability and differentiation comparable to, or even better than, those on commonly used poly-L-lysine coated glass coverslips. The polymer brushes were then patterned *via* UV photolithography techniques to provide specially designed surface features with different sizes (varying from 2  $\mu\text{m}$  to 200  $\mu\text{m}$ ) and orientations (horizontal and vertical). Protein absorption experiments and hippocampal neuronal cell culture tests on the brush patterns showed that both protein and neurons can adhere to the patterns and therefore be guided by such patterns. These results also demonstrate that, because of their unique chemical composition and well-defined nature, the developed polymer brushes may find many potential applications in cell-material interactions studies and neural tissue engineering.

### Keywords

Polymer brushes; surface-initiated atom transfer radical polymerization; acetylcholine functionality; photolithography; neuronal cell patterning

## 1. INTRODUCTION

In recent years, neural tissue engineering has rapidly emerged as a new field in central nervous system (CNS) therapeutics and has achieved much success.<sup>1</sup> It applies tissue engineering principles to therapy, and focuses on regulation of cell behavior and tissue progression through the implantation of foreign substances. The implanted materials have to meet certain criteria to be successfully integrated into the surrounding biological environments. First of all, they should provide appropriate chemical and physical properties that are analogous to the natural extracellular microenvironments to support neuronal cell adhesion and growth, such as proper biochemical factors, wettability, degradation rate,

\*Corresponding Author Department of Materials Science and Engineering, Cornell University, Ithaca, NY 14853. Tel: +1 607 255 8417; Fax: +1 607 255 2365. cko3@cornell.edu.

porosity, and mechanical strength. Synthetic polymers are attractive for this research area because many of their properties are controllable and they can also be further optimized for particular applications. To date, a wide variety of synthetic polymers with various chemical functionalities have been explored for CNS applications,<sup>2,3</sup> some successful examples include PEG based materials, polyglycolic acid (PGA), and biomaterials containing functional bioactive components such as extracellular matrix (ECM) peptides and neurotrophic factors. Surface topography of the materials has been considered as another important factor that can directly influence neuron cellular behaviors, including adhesion, morphology, proliferation and differentiation.<sup>4,5</sup> Recently, there has been a surge of interest in creating patterned surfaces with microelectronics techniques to provide welldefined surface architecture and geometry, thereby achieve a high-degree control over cell adhesion and induce formation of neuronal networks on material surfaces. For example, photolithographic techniques have been used for patterning neuronal cells at sub-cellular dimensions,<sup>6,7</sup> and offer valuable new approaches for more fundamental studies of *in vitro* cell surface and cell-cell interactions.

The application of micro-fabrication technology in neuronal tissue engineering has also stimulated interest and experiments in the development of a wide range of prosthetic and medical devices. However, many electrodes are limited in their long-term effectiveness due to their inability to effectively and chronically interface with host nervous tissue. Thus, research has been actively developing strategies to introduce thin films of synthetic polymers to tailor surface characteristics of those devices while maintaining their bulk properties. Polymer solution deposition, spin or spray coating, and self-assembled monolayers (SAM) are most commonly used methods to prepare polymer thin films.<sup>8</sup> Alternatively, polymer chains can be covalently attached to the substrate at one end to form polymer brushes.<sup>9</sup> The advantage of polymer brushes over other surface modification methods is their excellent mechanical and chemical robustness, at the same time offer unique physical properties to the substrates since the other end of the polymer chains may freely move in solution. They also provide a high degree of synthetic flexibility toward the introduction of a variety of functional groups. In particular, surfaceinitiated atom transfer radical polymerization (SI-ATRP) reactions can tolerate a wide range of functional monomers and be conducted under less stringent experimental conditions, they have become the most popular routes to control the functionality, density and thickness of the polymer brushes with near molecular precision.<sup>10</sup> Many specific material properties can be further amplified by this surface preparation method. For example, poly(PEGMA) brushes prepared by SI-ATRP method have been demonstrated to be “nonfouling.”<sup>11</sup> The brushes have been shown to be exceptionally resistant to the adsorption of adhesive proteins such as fibronectin as well as protein complexes and concentrated protein mixtures such as fetal bovine serum (FBS), and to be able to prevent nonspecific cell adhesion for up to 30 days.

Another advantage of using polymer brushes over other coating methods is their compatibility with a wide range of micro- or nano-fabrication techniques that can be used for cell patterning. The choice of chemical composition on the patterns is critical for both background (or off-pattern region) and foreground (or on-pattern regions).<sup>4,7</sup> Non-adhesive materials, such as PEG based materials, were often used for the background filling to reduce nonspecific protein adsorption and cell adhesion. For the on-patterned region, rationally designed biomaterials with proper information contents and functionalities should be present in order to direct appropriate cellular activities, and one way to achieve such bioactivity is to integrate biomolecules into polymers. For example, surface-tethered neurotransmitters can activate the corresponding cellular receptors and induce specific neuronal responses.<sup>12-14</sup> In particular, acetylcholine (ACh, 2-Acetoxy-N,N,N-trimethylethanaminium) is one of the most important and interesting neurotransmitters in CNS, and has shown to regulate

neuronal development and enhance neurite outgrowth *in vivo*.<sup>15</sup> Structural mimetics of acetylcholine, such as aminoethyl acetate and dimethylaminoethyl methacrylate (DMAEMA), have been used to prepare soluble polymers. Those tertiary amines can be protonated and become positively charged at neutral pH, therefore provide properties similar to acetylcholine and promote neurite sprouting and extension of dorsal root ganglia (DRG)<sup>14</sup> or rat hippocampal neurons.<sup>16</sup> In other studies, permanently positively charged quaternary ammonium salts (QAS), such as (2-methacryloyloxy)ethyl-trimethylammonium chloride (MAETAC), have been used to provide chemical structures that more closely mimic that of acetylcholine,<sup>13,17</sup> and to improve neuronal cell attachment on surfaces. The approaches of using MAETAC are better alternatives because they are pH-independent and can represent the entire functional structure of acetylcholine in a polymer system. However, those charged molecules have to be used at low concentration and combined with more biocompatible components (e.g., polyethylene glycol fumarate, poloxamine, PHEMA or PEG) due to their acute cytotoxic effects.<sup>13,14,16,18,19</sup> In addition, in those previous studies, acetylcholine functionalities and their structural mimetics were either embedded in cross-linked hydrogels or incorporated in linear soluble polymers. Those polymers often lack flexibility and/or stability in CNS applications, especially when used as prosthetic device coatings. Unfortunately, to the best of our knowledge, there are currently no acetylcholine and PEG based copolymers prepared in polymer brush forms for neuronal cell studies, despite many advantages that polymer brushes can offer in this area, such as stability, uniformity, well controlled structures, and readiness to be patterned using photolithography techniques.

In this study, to further explore the potential of biomimetic materials containing acetylcholine functionalities in neural tissue engineering, particularly the possibility of modulating the attachment and growth of primary hippocampal neurons on those synthetic materials, we prepared poly(PEGMA-*ran*-MAETAC) random copolymer brushes using SI-ATRP reactions on silicon substrates. The chemical structure of synthesized polymer brushes includes tethered “bio-active” acetylcholine segments (2-acetoxy-N,N,N-trimethylethanammonium) to alter the “non-fouling” properties of poly(PEGMA) polymer brushes and to promote neuronal cell attachment, and the “bio-inert” poly(ethylene glycol) units in the polymer brushes were chosen to provide good biocompatibility and regulate nerve cell interaction with the surfaces. The aim of this study is to determine the effects of the acetylcholine functionalized PEG polymer brushes and their topography on neuronal cell behaviors. The knowledge gained from the study could provide us with a better understanding of cell-surface interactions on this specific type of material.

## 2. MATERIALS AND METHODS

### 2.1. Materials

To prepare poly(PEGMA-*ran*-MAETAC) brushes from PEGMA and MAETAC monomers and pattern the brushes, allyl 2-bromo-2-methylpropionate, chlorodimethylhydrosilane, Pt on activated carbon (10 wt %), triethylamine, CuBr, CuBr<sub>2</sub>, 2,2'-bipyridine, poly(ethylene glycol) methacrylate (PEGMA, Mw = 360) and a 75% w/v aqueous solution of 2-methacryloyloxyethyl trimethylammonium chloride (MAETAC) were purchased from Sigma-Aldrich. 2-methoxy(polyethylenoxy)propyltrichlorosilane (PEG-silane, CH<sub>3</sub>O(CH<sub>2</sub>CH<sub>2</sub>O)<sub>6-9</sub>(CH<sub>2</sub>)<sub>3</sub>SiCl<sub>3</sub>, 90%) was purchased from Gelest, U.S.A. Silicon wafers were purchased from Platypus Technologies, U.S.A. For protein absorption tests, hippocampal neuronal culture and staining experiments, FITC-labelled BSA, poly-L-lysine (PLL), paraformaldehyde, phosphate buffered saline (PBS, pH 7.4), normal goat serum (NGS), 0.1% Triton-X100, mouse monoclonal anti-β-tubulin III antibodies were purchased from Sigma-Aldrich. Neurobasal-A, B27, trypsin were purchased from Gibco, U.S.A. LIVE/DEAD viability/cytotoxicity assay kit was from Invitrogen, U.S.A. Alexa Fluor® 488 goat anti-mouse IgG and Alexa Fluor® 568 goat anti-rabbit IgG, and DAPI were obtained from

Molecular Probes, U.S.A. All solvents used were purchased from Sigma-Aldrich, and all the chemicals were used without further purification unless otherwise noted.

## 2.2. Preparation of Poly(PEGMA-ran-MAETAC) Brushes through SI-ATRP

ATRP initiator (3-(chlorodimethylsilyl)propyl 2-bromo-2-methylpropionate was synthesized and immobilized to substrates as previously reported<sup>20</sup>. To prepare polymer brushes, silicon wafers covered with initiator were cut into 1 × 2 cm pieces and placed in a dry Schlenk tube. CuBr (57.4 mg, 0.4mmol), CuBr<sub>2</sub> (9.0 mg, 0.04mmol), and anhydrous 2, 2'-bipyridine (156.8 mg, 1.0 mmol) were added to another dry Schlenk tube equipped with a magnetic stir bar. Both flasks were evacuated and purged with nitrogen three times, 10–15 min each time. PEGMA (3.6 mL, 11.0 mmol) and MAETAC (0.4 mL, 1.6 mmol) monomers were flowed through the inhibitor removal column (Aldrich Chemical Co.) before mixing with isopropanol (3.6 mL) and DI water (2.4 mL). The reaction mixtures were then bubbled with nitrogen gas for at least 30 min and transferred into the Schlenk tube with copper catalysts using a clean cannula. The mixture was stirred at room temperature under nitrogen for about 10 min before being transferred into the other Schlenk tube with initiator attached silicon substrates. Polymerization was carried out at room temperature for 5 h, after which the substrates were taken out of the solution, rinsed thoroughly with DI water and isopropanol, and blown dry with nitrogen gas.

## 2.3. Polymer Brush Surface Characterization

Water contact angles were measured using a contact angle goniometer (Ramé-Hart NRL C.A. model 100–00 115) at room temperature. Three measurements from different locations on the sample were recorded, and the data was reported as Mean ± SD. The thickness of polymer brushes was measured using an imaging ellipsometer (Nanofilm EP3) at a fixed angle of incidence (65 degrees) and wavelength (401–711 nm) mode. A Cauchy model/silicon oxide/silicon stack model was used to fit the data, in which the Cauchy parameter of poly(methyl methacrylate) (PMMA) represented the polymer brush. Three different points were measured for each sample and the average and standard deviation were calculated. The topography of the polymer brush modified silicon surfaces was measured by atomic force microscopy (AFM) using a Dimension Icon AFM (Bruker Corporation, Karlsruhe, Germany). An area of 5×5 μm was scanned using tapping mode, the drive frequency was 357.5 KHz, and the voltage was between 4.0 and 4.5 V. The drive amplitude was 64.1mV and the scan rate was 0.996 Hz. An arithmetic mean of the surface roughness (*R<sub>a</sub>*) was calculated from the roughness profile determined by AFM.

Polymer brush-modified silicon wafers were also characterized by attenuated total reflectance Fourier transform infrared (ATR-FITR) spectroscopy using a VERTEX 80v and PIKE technologies VeeMAX II accessory equipped with a germanium crystal. A nitrogen cooled MCT detector was used and a ZnSe polarizer was set for parallel (p) polarization. Before collecting data, the system was left in vacuum for 10 min to minimize signal noise from air. The spectra were measured under reduced pressure (less than 3 hPa) and data was collected using 1024 scans with 4 cm<sup>-1</sup> resolution. A spectrum from a freshly cleaned silicon wafer was used to determine the background signal.

X-ray photoelectron spectroscopy (XPS) measurements were performed using a Kratos Axis Ultra Spectrometer (Kratos Analytical, Manchester, UK) with a monochromatic Al K $\alpha$  X-ray source (1486.6 eV) operating at 225 W under a vacuum of 1.0 – 10<sup>8</sup> Torr. The pass energy of the analyzer was set at 20 eV and the spectra were analyzed using Casa XPS v. 2.3.14 software. The C-C peak at 285 eV was used as the reference for binding energy calibration. Near Edge X-Ray Absorption Fine Structure (NEXAFS) spectroscopy experiments were carried out on the U7A NIST/Dow materials characterization end station

at the National Synchrotron Light Source at Brookhaven National Laboratory (BNL). The details of this experimental geometry and illustration of the setup have been reported previously.<sup>21</sup> The peak position of the lowest  $\pi^*$  phenyl resonance from polystyrene (285.5 eV) was used to calibrate the photon energy.

#### 2.4. Patterning of Polymer Brushes by Photolithography

Poly(PEGMA-*ran*-MAETAC) brushes were patterned on silicon surface using photolithography as shown in Figure 4. The silicon wafer was treated with freshly prepared piranha solution for 1 h and then cleaned with water, isopropanol and blown dry under nitrogen gas. A self-assembled monolayer of PEG silane was used as a non-adhesive backfill for the pattern. The clean wafer was immersed in a 1% (v/v) solution of the PEGylated silane in anhydrous toluene containing catalytic amounts of triethylamine overnight at room temperature, followed by rinsing with anhydrous ethanol and drying with nitrogen. After PEG-silane deposition, S1813 positive tone photoresist (Shipley) was spin-coated onto the PEG-functionalized silicon wafer at 3000 rpm for 60 sec, and soft baked at 115 °C for 1 min, resulting in a film about 1  $\mu$ m thick. The wafer was then exposed to UV light ( $\lambda = 415$  nm, 17 mW/cm<sup>2</sup>) through patterned photo mask for 2 sec using an ABM contact aligner. After development in a tetramethylammonium hydroxide solution (AZ 300 MIF), the exposed PEG regions were etched using a Harrick oxygen plasma cleaner (PDC-32G) for 2 min.

The PEG backfilled substrate was immersed in a hexane solution of the ATRP initiator (5 mM) with catalyst amount of pyridine. The reaction was carried out at room temperature under the protection of nitrogen for 24 h. The remaining photoresist was stripped off using acetone. The initiator immobilized wafer was then cleaned with ethanol, water and acetone sequentially, and blown dried with nitrogen. The patterned surface with initiator was used immediately in the next step of surface-initiated polymerization to grow polymer brushes as described in the previous section (Sec. 2.2).

#### 2.5 Protein adsorption on patterned polymer brushes

Protein adsorption of the patterned surfaces was tested against FITC-labeled BSA (0.1 mg/ml in PBS buffer) at room temperature. After 2 hours the patterned silicon wafer was taken out of protein solution and rinsed with deionized water and immediately analyzed with a fluorescence microscope (BX51, Olympus, Japan). Images were recorded using a Cool Snap hx CCD camera (Roper Scientific) with an LMPlan FI 10x dry objective lens (excitation, 470 nm; emission, 525 nm). The fluorescence intensities were processed with Image-Pro Plus (Media Cybernetics, Inc., Bethesda, MD) software.

#### 2.6. Primary Mouse Hippocampal Neuronal Cell Culture

Animal experiments were carried out according to the institutional animal care procedures. The polymer brush coated wafer samples were sterilized in 75% ethanol 5 h before use. Primary hippocampal neuronal cultures were prepared through enzymatic dissociation of hippocampi removed from postnatal day 0 mouse pups as previously described.<sup>13</sup> Briefly, hippocampi were dissected out, chopped into small pieces and digested with 0.125% trypsin. After digestion, a single cell suspension was prepared by trituration. The cells were plated at a density of 40,000 cells/mL onto the brush samples, and then cultured in Neurobasal-A medium supplemented with B27 and maintained for 3 days at 37°C before fixation. PLL coated glass slides were used as control in these experiments and followed the same cell culture procedure. All cell culture experiments were carried out in 24 well culture plates, and each experiment repeated 3 times.



## 2.7. Cell Viability, Immunostaining, and Statistical Analysis

Cell viability was measured using the standard LIVE/DEAD Viability/Cytotoxicity Assay Kit from Invitrogen. After 3 days of culture, each brush sample was placed in 1 mL growth media with 0.5  $\mu$ L calcein and 2  $\mu$ L ethidium homodimer, and incubated at 37°C for 20 min. Cell attachment and viability were visualized using an Eclipse 800 (Nikon Instruments Inc., Melville, NY) fluorescence microscope. Five random fields of each sample were imaged on both green and red channels and the number of live and dead cells was counted manually for each image. The number of live cells divided by the total number of live and dead cells was defined as the fractional viability.

All immunostaining experiments were carried out at room temperature. Cells on polymer brush samples and PLL coated glass cover slides were fixed after three days of culture with 4% paraformaldehyde in PBS buffer. The samples were then prepared for immunostaining by blocking and permeabilizing in 10% NGS and 0.1% Triton-X100 in PBS (v/v, PBS-T) for 1 h, followed by incubation with the primary antibodies of monoclonal mouse anti- $\beta$ -tubulin III (1:1000) and polyclonal rabbit anti-GFAP (1:1000) (diluted in PBS-T buffer containing 2% NGS) for 2 h. The cells were then incubated for 1 h with secondary antibodies AlexaFluor<sup>®</sup>488-conjugated goat anti-mouse IgG (1:1000) and Alexa Fluor<sup>®</sup>568-conjugated goat anti-rabbit IgG (1:1000) diluted in PBS-T containing 2% NGS, followed by incubation with nuclear counterstain with DAPI (1:1000) in PBS buffer for 5 min at room temperature. After thoroughly rinsing with PBS buffer, cell culture samples were imaged using the fluorescence microscope. The number of cells was counted manually for each image using ImageJ to determine the number of neurons and astrocytes at each random field. Estimation of neurite outgrowth was determined by manually counting intersections of neurites with test lines of an unbiased counting frame (horizontal lines, area per point of 0.5 inch<sup>2</sup>), the resulting ratio of intersections of neurites to neuron cells was calculated as relative neurite length<sup>22</sup>. Each experiment was repeated three times. Statistical analyses were performed by one-way ANOVA followed by Turkey post hoc test. Results were considered statistically significant if  $p < 0.05$  and marked with asterisks.

## 3. RESULTS

### 3.1. Preparation and Characterization of Poly(PEGMA-*ran*-MAETAC) Brushes

Poly(PEGMA-*ran*-MAETAC) brushes were synthesized on silicon substrates using the surface initiated atom transfer radical polymerization (SI-ATRP) method, and only small amount of MAETAC was used (10% v/v) to prepare the polymer brushes to avoid its cytotoxic effects.<sup>13,18</sup> Moreover, polymer brushes with different amounts of MAETAC have been prepared (40%, 30%, 20%, and 10%) and tested in the initial studies (data not shown), and samples with 10% MAETAC showed the best results in neuronal cell culture experiments. The reaction was carried out in two steps (Figure 1A). In the first step, ATRP initiator was covalently attached to a clean silicon surface freshly treated in piranha solution to form a self-assembled monolayer (SAM). The modified surface became more hydrophobic compared to the bare silicon surface (static water contact angles are less than 10°), with the static water contact angles of 65° (SD  $\pm$  2°) after the reaction. In the second step, random copolymerization of PEGMA and MAETAC monomers was carried out under oxygen-free conditions at room temperature, and CuBr/bipyridine was used as a catalyst. After 5 hours of reaction at room temperature, the surfaces were cleaned with water and isopropanol. Static water contact angle measurements showed that the brush modified surfaces are more hydrophilic compared to the ATRP initiator modified surfaces in the first reaction step, with water contact angles of 47° (SD  $\pm$  3°). Ellipsometry measurement showed that the brush thickness was 21  $\pm$  2 nm. An AFM microscope was used to investigate the surface topography and roughness (Figure 1B). The polymer brushes gave a

relatively smooth surface and the arithmetic average roughness ( $R_a$ ) measured over an area of  $5 \times 5 \mu\text{m}$  was estimated to be  $\sim 3 \pm 1.8 \text{ nm}$ .

ATR-FTIR was used as an additional tool to characterize the substrate surface (Figure 2A). The presence of a strong absorption band at  $1724 \text{ cm}^{-1}$  is characteristic of a saturated ester carbonyl group stretching ( $-\text{C}=\text{O}$ ), while the absorption region at  $1121 \text{ cm}^{-1}$  arises from the stretching of the  $\text{C}-\text{O}-\text{C}$  group in PEG units. The band at  $2869 \text{ cm}^{-1}$  is an aliphatic  $-\text{C}-\text{H}$  stretching vibration, and the broad absorption at  $3200\text{--}3600 \text{ cm}^{-1}$  corresponds to the  $-\text{OH}$  absorption on the PEG unit. Overall, the FTIR spectrum provided evidence that supports the formation of the target polymer brush on the silicon surface.

To fully characterize the surface chemistry of poly(PEGMA-*ran*-MAETAC) brushes, the presence of the brushes on the silicon surface was also evaluated by XPS analysis. An XPS wide scan examination and  $\text{C}1s$  core-level spectra of the brush surfaces are shown in Figure 2B. The  $\text{C}1s$  core-level spectrum (Fig. 2B, right) can be curve-fitted with three peak components having binding energies at 284.5, 286.2, and 288.5 eV, attributable to the  $\text{C}-\text{C}$ ,  $\text{C}-\text{O}$ , and  $\text{O}=\text{C}-\text{O}$  species, respectively. The binding energy near 400.0 eV shown in the XPS wide scan (Figure 2B left) corresponds to quaternized nitrogen. In addition, NEXAFS has been described as a powerful tool to characterize a nitrogen containing compound<sup>23</sup>. Figure 2C shows the normalized carbon and nitrogen K edge NEXAFS spectra of the brush. The small resonance peak near 287.7 eV can be attributed to the  $\text{C } 1s \rightarrow \pi^*_{\text{C}=\text{O}}$  signal. The characteristic signals at 291.4 eV is the  $\text{C } 1s \rightarrow \sigma^*_{\text{C}-\text{H}}$ , and a strong peak at 295.4 eV can be easily seen for this surface, they are indicative of the  $\text{C } 1s \rightarrow \sigma^*_{\text{C}-\text{O}}$  resonances, demonstrating the PEG containing side chain groups dominating the surface<sup>21,24</sup>. The tall peak at 412.8 eV corresponds to the  $\text{N } 1s \rightarrow \sigma^*_{\text{C}-\text{N}}$  transition in the nitrogen K edge. Spectra from four different angles ( $20^\circ$ ,  $60^\circ$ ,  $90^\circ$ ,  $120^\circ$ ) were found to be identical and indicate that there is no specific orientation on this random polymer brush surface, in other words, the polymer brushes provide a surface with uniform chemical composition.

### 3.2. Polymer Brush Modified Silicon Surfaces for Hippocampal Neuron Cell Culture

Dissociated mouse hippocampal neurons were plated on the polymer brush surfaces. After 3 days of culture, cellular viability was assessed *via* the LIVE/DEAD cell viability/toxicity assay (Figure 3A and 3C). Neuronal cells maintain 75.6 % cell viability on the brush surface, which is also comparable to standard PLL coated glass coverslips under the same culture condition (77.6%). Results of double-label immunocytochemistry (Figure 3B and 3D) showed that the poly(PEGMA-*ran*-MAETAC) brushes favor the attachment and outgrowth of neurons over astrocytes, with 48.1 neurons and only 15.5 astrocytes per random field, giving an average of 3.1 times of more neurons than astrocytes in a random field. This is also comparable with neuronal cells on PLL coated glass surfaces cultured under the same conditions (average 4.3 neuron/astrocytes).

Morphometric analysis of neurite outgrowth on surfaces is a useful approach to investigate the mechanisms regulating differentiation of neurons and their connections. In this work, a simple procedure based on stereological principles was applied to morphometric analysis of cell culture on both polymer brushes and PLL modified surfaces.<sup>22</sup> Results of the analysis have showed that the hippocampal neurons cultured on the brush surfaces possessed the average mean neurite length per cell significantly longer than those cultured on the PLL modified control surfaces (Figure 3E), with average 2.98 intersections/cell on a polymer brush surfaces and 2.42 intersections/cell on a PLL coated surfaces, respectively.

### 3.3. Protein Absorption and Neuronal Cell Patterning on Poly(MAETAC-*ran*-PEGMA) Brushes

Patterned polymer brushes have been successfully prepared using photolithography method (Figure 4A). The pattern was designed to present straight lines of different widths (2  $\mu\text{m}$  to 200  $\mu\text{m}$ ) on the surface, and all the straight horizontal lines were also connected to each other at one end to provide curves and give another orientation (vertical). Figure 4B shows the ellipsometry mapping picture of the patterned brushes. The thickness of the patterned brushes was  $20 \pm 3$  nm using the ellipsometry method described in section 2.3. Incubating the patterned brush surface in FTIC-BSA solution demonstrated that protein can be nicely patterned on the substrate. Fluorescence imaging clearly shows that FTIC-BSA was absorbed on the brush patterns but not on the PEG SAM background (Figure 5A), indicating the difference between acetylcholine/PEG modified surfaces and PEG alone modified surfaces.

Hippocampal neurons can also be guided along the brush patterns. The images in Figure 5B provide evidence that geographic cues are also important factors in determining neuronal cell behaviors in this system. Neuronal growth is largely confined to poly(PEGMA-*ran*-MAETAC) brushes coated paths, while the degree of attachment and alignment of neurite outgrowth was dependent on pattern widths. There is a strong visual impression that 2  $\mu\text{m}$  and 5  $\mu\text{m}$  lines seem too small to allow neuronal attachment (not shown, patterned lines cannot be identified using fluorescence microscopy), as no specific attachment and alignment of neurons were observed on those lines. A few cells were attached to 12  $\mu\text{m}$  lines, but they hardly formed any connection with other cells, neither have they developed long processes along the lines. However, cells seemed to prefer to attach to the lines wider than 12  $\mu\text{m}$ . On 25  $\mu\text{m}$  lines, neurite elongation was precisely oriented along the tracks of the brushes, and their processes intermingle with those of other neurons along the line. On lines with widths equal or great than 50  $\mu\text{m}$ , more neurons attached to brushes, and neurites showed more significant outgrowth, and they form a meshwork within the lines. Networks become more complicated with the increase of the line widths. On 200  $\mu\text{m}$  lines, cells grew in a manner similar to that of unpatterned brush surfaces, although cells are still strictly confined by the border of the pattern.

## 4. DISCUSSION

### 4.1 Polymer Brush Preparation and Characterization

In this study, biomimetic random copolymer brushes of neurotransmitter acetylcholine derivatives (MAETAC) and biocompatible PEG were prepared through SI-ATRP reaction. Before the polymerization reaction, a bromoester initiator was covalently linked to a silicon surface to form a self-assembled monolayer (SAM). This step of surface preparation provided a simple and reliable method to covalently tether the organic layer on the substrate. The silicon surface was used as a model substrate, but the technique can also be easily employed on other commonly used substrates such as glass, gold, silver, copper and platinum surfaces or silicon oxide based polymeric substrates.<sup>8,10</sup> The following polymerization of monomers was carried out in water/isopropanol solution to form polymer brushes on the surface. Related to this method, previous work<sup>25</sup> on SI-ATRP-polymerized poly(PEGMA) homopolymer brushes in water showed that chain growth from the surface was a controlled “living process”, and the thickness of poly(PEGMA) brushes was a function of polymerization time. However, certain degrees of rapid chain termination on the surface in the early stage of polymerization were observed, and this phenomenon was followed by slow bimolecular coupling or disproportionation reactions that consume the active chains. Longer reaction times (more than 12 h) also introduced chain transfer from surface-active sites to the reaction solution. In another study, for “non-fouling”



poly(OEGMA) polymer brushes prepared in water/methanol solvent mixtures,<sup>11</sup> a linear relationship of brush thickness against reaction time was found for a reaction time less than 2 h. For a longer reaction time, a deviation from a linear fit to an exponential fit was observed, and after 5 h of reaction time, the thickness of the polymer brushes reached a value of roughly 50 nm. The authors explained this phenomenon could be caused by slow leakage of oxygen into the reaction system and/or increased steric interference to chain growth for longer polymer brushes. In the same study, brush density was also varied to prepare a binary brush system of poly(OEGMA), and the thickness of the polymer brush reached a steady state value of 20 nm. Beyond this value no further increase in film thickness was observed. Furthermore, the homopolymer brushes of poly(MAETAC)<sup>26</sup> have also been prepared through ATRP reaction. The reaction was carried out in methanol, and it has been shown that transesterification of quaternary amine methacrylates can take place during methanolic ATRP. However, such transesterification can be avoided when methanol is replaced by isopropanol (IPA) because a secondary alcohol is less prone to ester interchange. In the present work, water/IPA was chosen as solvent to prepare polymer brushes containing both PEGMA and MAETAC units. The reaction was terminated after 5 h, and gave a uniform layer of brushes on the substrate surface. Polymer brush thickness with reaction time was not investigated in this study, since neuronal cells can respond to proper surface chemistry even at 1 nm thickness,<sup>27</sup> and the effect of brush thickness on cell culture is not the focus of this study. However, thickness of the polymer brushes could influence many cell behaviors such as attachment, survival and growth. Future studies that systematically investigate the thickness profiles may lead to better understanding of the cell-surface interactions on these materials. The brushes prepared in this work are relatively thin (~ 21 nm), which is ideal for biomedical device coating applications, where the brushes can be used to optimize the surface chemical properties of the devices without dramatically changing the shape, size and mechanical properties of the devices.

The resulting poly(MAETAC-*ran*-PEGMA) brushes exhibited water contact angles ( $47^\circ \pm 3^\circ$ ) similar to the poly(PEGMA) brush prepared in water ( $44^\circ$ ),<sup>25</sup> and it may be concluded that including a small amount of acetylcholine functionality in the polymer brush does not significantly affect the hydrophobicity of the poly(PEGMA) surfaces. Maintaining the appropriate hydrophobicity in the polymer brush might be important to retain the biocompatibility/non-toxic properties of the poly(PEGMA) brush, since surface hydrophobicity has consequently been widely cited as a key factor in determining protein and cell-surface interaction.<sup>28</sup> FT-IR, XPS and NEXAFS data have also confirmed the surface chemistry of the brushes, these results, together with AFM measurement of the surface, suggested that random copolymerization of PEGMA and MAETAC *via* SI-ATRP gave chemically uniform, welldefined polymer brushes on the silicon surface.

#### 4.2 Mouse Hippocampal Neuronal Cell Attachment and Neurite Outgrowth on Polymer Brushes

Previous studies have shown that pure PEG-based biomaterials can cause poor nerve cell survival due to its effect on cell adhesion, and the presence of MAETAC at high concentration may also lead to a large and acute loss of cell viability because of its cytotoxicity.<sup>13,18,19</sup> The polymer brushes reported here contain low concentration of MAETAC in order to both maintain the biocompatibility of the polymer brushes, while providing tethered bioactive neurotransmitter components. The viability/toxicity assay of mouse hippocampal cells cultured on the polymer brush surfaces showed that, incorporating acetylcholine into poly(PEGMA) polymer brushes at this concentration can totally alter the “non-sticky” property of the poly(PEGMA) homopolymer brushes and dramatically improve neuronal cell attachment and survival (75.6 % viability)(Figure 3A and 3C), even though much of the material is PEG. Immunocytochemistry also showed that the brush surfaces

permitted the growth of neurons and astrocytes comparable to that on PLL coated glass slides (Figure 3E). In addition, hippocampal neurons on the brush surfaces exhibited the healthy cellular growth morphology, possessing multiple dendrites and long axons. The relative length of neurites on a polymer brush surface is significantly longer than that on PLL coated glass substrates when the cells are cultured under the same conditions. As compared to PLL coatings, poly(PEGMA-*ran*-MAETAC) brushes are stable since they are covalently linked to the substrates. The polymer brush samples can still support neuronal attachment and growth after 4 months when stored at room temperature (longer storage time has not been tested), while PLL coatings are physically absorbed to the surfaces and usually must to be prepared freshly. Also, polymer brushes offer synthetic flexibility and provide opportunities to introduce other interesting functional groups or bioactive molecules through free hydroxyl terminal groups. More importantly, poly(PEGMA-*ran*-MAETAC) brushes preparation is compatible with modern photolithographic techniques for cell patterning. All these properties provides advantages for poly(PEGMA-*ran*-MAETAC) brushes over PLL coatings for specific cell studies and neuronal engineering applications. The mechanism of neuronal cell attachment and neurite outgrowth on the polymer brushes is currently unknown and it is an important topic that is worth future investigation. However, it is possible that acetylcholine functionalities in the polymer might mediate the effects of acetylcholine receptors of neurons;<sup>14</sup> alternatively, the positively charged polymer surfaces may lead to changes in the ion flux on the cell membrane.<sup>18</sup> This situation can be further complicated by protein adsorption to the surface prior to cell attachment, as described in the protein absorption test on polymer brushes (Sec. 3.3.). During experiments we also observed that neurons attached to the polymer brush surface are not as strongly attached as those on the PLL coated surfaces, so that cells were more easily washed away and the processes can also be broken during washing steps if it is not carefully handled. This is probably caused by the lower positive charge density on the surface and non-fouling properties of PEG units present in the brushes. In light of this evidence, we hypothesize that the weaker interaction between the surface and neuronal cells allows cells to differentiate easily, while high positive charge density leads to strong interaction which can retard neuronal cell attachment on the surfaces and hinder further differentiation and spreading. Comparing the effect of interaction forces to the neuronal cell growth and morphology on this type of synthetic materials is currently a focus of our research.

### 4.3 Protein and Neuronal Cell Patterning

In this work, a specifically designed pattern was introduced to the silicon substrate surface through UV photolithographic techniques. Although the current patterned silicon wafers were not intended to be used *in vivo*, the goal of this study was to develop methods and establish knowledge that may be applied to prepare more sophisticated micro-devices that are specifically designed for *in vivo* applications in the future. The pattern incorporates both surface chemical and topographic cues in one single visual field. Besides obvious reasons of time-saving and cost-effective character, the pattern provides a unique and convenient platform for cell-surface interaction studies. In details, two different types of chemical signals were presented on those patterns: the PEG polymer brushes with acetylcholine functionalities formed the on-pattern features, and PEG silane self-assembled monolayer (PEG-SAM) was used to backfill the patterns to provide non-adhesive off-pattern regions. It also served as negative control surface that highlights the differences between acetylcholine functionalized poly(PEGMA) brush surfaces and surfaces containing only PEG groups for neuronal cell adhesion and growth. The pattern also provides features at different sizes (2  $\mu\text{m}$  to 200  $\mu\text{m}$ , 100 times difference) and directions (horizontal *vs.* vertical). To test the pattern, biomacromolecules such as BSA protein was used and Figure 5A showed that, compared to PEG-SAM background, BSA protein absorption is much higher on pattern features formed by polymer brushes. Protein absorption on the patterns could be explained

by the positively charged nature of acetylcholine functionalities in the polymer brushes, since the pI of BSA is around 4.7, and in PBS solution BSA is negatively charged, which enhances the absorption of a protein on the positively charged brush surfaces. This is a significant change from poly(PEGMA) homopolymer brushes, as previously reported that poly(PEGMA) brushes resist non-specific binding and are exceptionally resistant to the adsorption of “sticky” proteins.<sup>11</sup> Protein absorption to the brush surface can also be the cause of improved “cell-surface” interactions on this type of materials, since in serum-containing culture medium, numerous species of protein molecules and albumin can be deposited and presumably dominate the surface characteristics, ultimately lead to improved conditions for cell adhesion and differentiation.<sup>8,29</sup>

The designed pattern has also proven to be effective to study cell reactions to surface chemical and physical cues under exactly the same culture condition. Results of hippocampal neuronal cell culture on the pattern showed that neuronal cells can recognize the surface chemical signal and prefer to stay on lines of polymer brushes containing acetylcholine functionalities (Figure 5B). The size and the orientation of the patterns are also major factors to determine the cell attachment and interaction. At feature sizes smaller than 12  $\mu\text{m}$ , neurons were not able to establish any connections, but they were tightly confined at 25  $\mu\text{m}$  lines. More complicated interaction and networks were formed at larger feature sizes (50–200  $\mu\text{m}$ ). It is also seemed that, in this specific pattern, neurons tend to stay on horizontal lines than vertical lines at the same size scale (100  $\mu\text{m}$ ), probably because horizontal is the dominate direction in this case. In addition, growth of extending neurites is strongly influenced by the patterns, resulting in cells with very different morphologies. For example, at line widths of 100  $\mu\text{m}$ , cells exhibited a star-shaped morphology, while at line width of 25  $\mu\text{m}$ , cells were extended as line-shaped. Results of this study are in agreement with previous studies on the patterning of neuronal cells on the surfaces with other chemical components, such as micro-stamped PLL,<sup>27,30</sup> phase mask interference lithography fabricated hydrogels,<sup>31</sup> and microfabricated patterns of parylene-C,<sup>32</sup> that the cell interaction and morphology of hippocampal neurons can be greatly affected by surface topographical cues. However, different from micro-stamped poly-lysine patterns,<sup>30</sup> poly(PEGMA-*ran*-MAETAC) brush patterns need larger pattern sizes to allow neuronal attachment and growth (25  $\mu\text{m}$  vs. 10  $\mu\text{m}$ ). This can also be explained by the charge density on the patterns, since positively charged acetylcholine is largely shielded with “non-fouling” PEG units in the polymer brushes, therefore, such brushes might not be as effective at guiding neuronal cells at smaller scales.

## 5. CONCLUSIONS

It is of great importance to develop biocompatible polymeric materials for neuroprosthetic device coatings and to effectively control growth of neurites for regeneration in the central nervous system. This study demonstrated that poly(PEGMA-*ran*-MAETAC) brushes can provide a simple and reliable way to prepare a permissive surface for neuronal cell culture and patterning on the substrates. Cells maintained high viability during the 3 day period of culturing on the polymer brushes, and neurite outgrowth was comparable or even better than that on the standard poly-L-lysine coated surfaces. The brushes can also be easily patterned through standard photolithography techniques. Both BSA protein absorption and hippocampal neuronal attachment and growth can be localized and guided by such brush patterns, and the pattern sizes and orientation greatly affect neuronal cell morphology and interaction. Because of the positively charged nature of the acetylcholine functionalities and the biocompatibility characteristics of PEG units, the random copolymer brushes may also find potential application to pattern other biomacromolecules such as negatively charged DNA, RNA molecules,<sup>33</sup> and to pattern other types of cells such as human endothelial cells.<sup>34</sup> The free hydroxyl terminal groups of the PEG units of the polymer brushes can also

be readily modified into various functional groups including chloride, amine, and carboxylic acid groups,<sup>25</sup> and covalently linked to other bioactive molecules for more specific neuronal engineering applications. In summary, with carefully designed patterns and introduction of functional specific bioactive molecules, the poly(PEGMA-*ran*-MAETAC) brushes may hold many potential in facilitating the study of neuronal physiologic processes where directed cell growth and migration is fundamental, and it may as well provide new solutions to problems involving cell - surface interactions and interfaces.

## Acknowledgments

We thank Dr. Youyong Xu for help with polymer brush preparation, Prof. E. J. Kramer, Dr. Warren Taylor and Dr. Daniel A. Fisher for XPS and NEXAFS analysis. We would like to acknowledge the use of the Microscopy and Imaging Facility at Cornell University, the Cornell Center for Materials Research (CCMR), the Cornell NanoScale Science & Technology Facility (CNF), and the Nanobiotechnology Center (NBTC) at Cornell University. We also acknowledge the assistance of the NHLBI DIR Light Microscopy Core Facility. This work was partially supported through the National Science Foundation (DMR-1105253) and through ONR grant (N000141110330), NIH (NSR01-044287), as well as the NHLBI Division of Intramural Research (P.Y. and H.M.G).

## REFERENCES

1. Constans A. *Scientist*. 2004; 18:40–42.
2. Zhong YH, Bellamkonda RV. *J. R. Soc. Interface*. 2008; 5:957–975. [PubMed: 18477539]
3. Aurand ER, Lampe KJ, Bjugstad KB. *Neurosci. Res.* 2012; 72:199–213. [PubMed: 22192467]
4. Khan S, Newaz G. *J. Biomed. Mater. Res. Part A*. 2010; 93A:1209–1224.
5. Smeal RM, Rabbitt R, Biran R, Tresco PA. *Ann. Biomed. Eng.* 2005; 33:376–382. [PubMed: 15868728]
6. Rohr S, Fluckiger-Labrada R, Kucera JP. *Pflug. Arch. Eur. J. Phy.* 2003; 446:125–132.
7. Craighead HG, James CD, Turner AMP. *Curr. Opin. Solid State Mater. Sci.* 2001; 5:177–184.
8. Senaratne W, Andruzzi L, Ober CK. *Biomacromolecules*. 2005; 6:2427–2448. [PubMed: 16153077]
9. Barbey R, Lavanant L, Paripovic D, Schuwer N, Sugnaux C, Tugulu S, Klok H-A. *Chem. Rev.* 2009; 109:5437–5527. [PubMed: 19845393]
10. Edmondson S, Osborne VL, Huck WTS. *Chem. Soc. Rev.* 2004; 33:14–22. [PubMed: 14737505]
11. Ma HW, Hyun JH, Stiller P, Chilkoti A. *Adv. Mater.* 2004; 16:338–341.
12. Saifuddin U, Vu TQ, Rezac M, Qian HH, Pepperberg DR, Desai TA. *J. Biomed. Mater. Res. Part A*. 2003; 66A:184–191.
13. Zhou Z, Yu P, Geller HM, Ober CK. *Biomaterials*. 2012; 33:2473–2481. [PubMed: 22196899]
14. Gumera CB, Wang Y. *Adv. Mater.* 2007; 19:4404–4409.
15. Whitteridge D. *J. Neurol. Neurosurg. Psychiatry*. 1948; 11:134–140. [PubMed: 18861112]
16. Tu Q, Li L, Zhang YR, Wang JC, Liu R, Li ML, Liu WM, Wang XQ, Ren L, Wang JY. *Biomaterials*. 2011; 32:3253–3264. [PubMed: 21303719]
17. Sosnik A, Sefton MV. *J. Biomed. Mater. Res. Part A*. 2005; 75A:295–307.
18. Dadsetan M, Knight AM, Lu LC, Windebank AJ, Yaszemski MJ. *Biomaterials*. 2009; 30:3874–3881. [PubMed: 19427689]
19. Schneider GB, English A, Abraham M, Zaharias R, Stanford C, Keller J. *Biomaterials*. 2004; 25:3023–3028. [PubMed: 14967535]
20. Dong R, Krishnan S, Baird BA, Lindau M, Ober CK. *Biomacromolecules*. 2007; 8:3082–3092. [PubMed: 17880179]
21. Dimitriou MD, Zhou ZL, Yoo HS, Killops KL, Finlay JA, Cone G, Sundaram HS, Lynd NA, Barteau KP, Campos LM, Fischer DA, Callow ME, Callow JA, Ober CK, Hawker CJ, Kramer EJ. *Langmuir*. 2011; 27:13762–13772. [PubMed: 21888355]
22. Ronn LCB, Ralets I, Hartz BP, Bech M, Berezin A, Berezin V, Moller A, Bock E. *J. Neurosci. Methods*. 2000; 100:25–32. [PubMed: 11040363]

23. Shard AG, Whittle JD, Beck AJ, Brookes PN, Bullett NA, Talib RA, Mistry A, Barton D, McArthur SL. *J. Phys. Chem. B.* 2004; 108:12472–12480.
24. Epps TH, DeLongchamp DM, Faselka MJ, Fischer DA, Jablonski EL. *Langmuir.* 2007; 23:3355–3362. [PubMed: 17291017]
25. Xu D, Yu WH, Kang ET, Neoh KG. *J. Colloid Interface Sci.* 2004; 279:78–87. [PubMed: 15380414]
26. Li YT, Armes SP, Jin XP, Zhu SP. *Macromolecules.* 2003; 36:8268–8275.
27. Ruiz A, Buzanska L, Gilliland D, Rauscher H, Sirghi L, Sobanski T, Zychowicz M, Ceriotti L, Bretagnol F, Coecke S, Colpo P, Ross F. *Biomaterials.* 2008; 29:4766–4774. [PubMed: 18819707]
28. Webb K, Hlady V, Tresco PA. *J. Biomed. Mater. Res.* 1998; 41:422–430. [PubMed: 9659612]
29. Chen H, Yuan L, Song W, Wu ZK, Li D. *Prog. Polym. Sci.* 2008; 33:1059–1087.
30. Branch DW, Wheeler BC, Brewer GJ, Leckband DE. *IEEE Trans. Biomed. Eng.* 2000; 47:290–300. [PubMed: 10743770]
31. Jang JH, Jhaveri SJ, Rasin B, Koh C, Ober CK, Thomas EL. *Nano Lett.* 2008; 8:1456–1460. [PubMed: 18393470]
32. Delivopoulos E, Murray AF, MacLeod NK, Curtis JC. *Biomaterials.* 2009; 30:2048–2058. [PubMed: 19138795]
33. Merdan T, Kopecek J, Kissel T. *Adv. Drug Delivery Rev.* 2002; 54:715–758.
34. Vanwachem PB, Hogt AH, Beugeling T, Feijen J, Bantjes A, Detmers JP, Vanaken WG. *Biomaterials.* 1987; 8:323–328. [PubMed: 3676418]



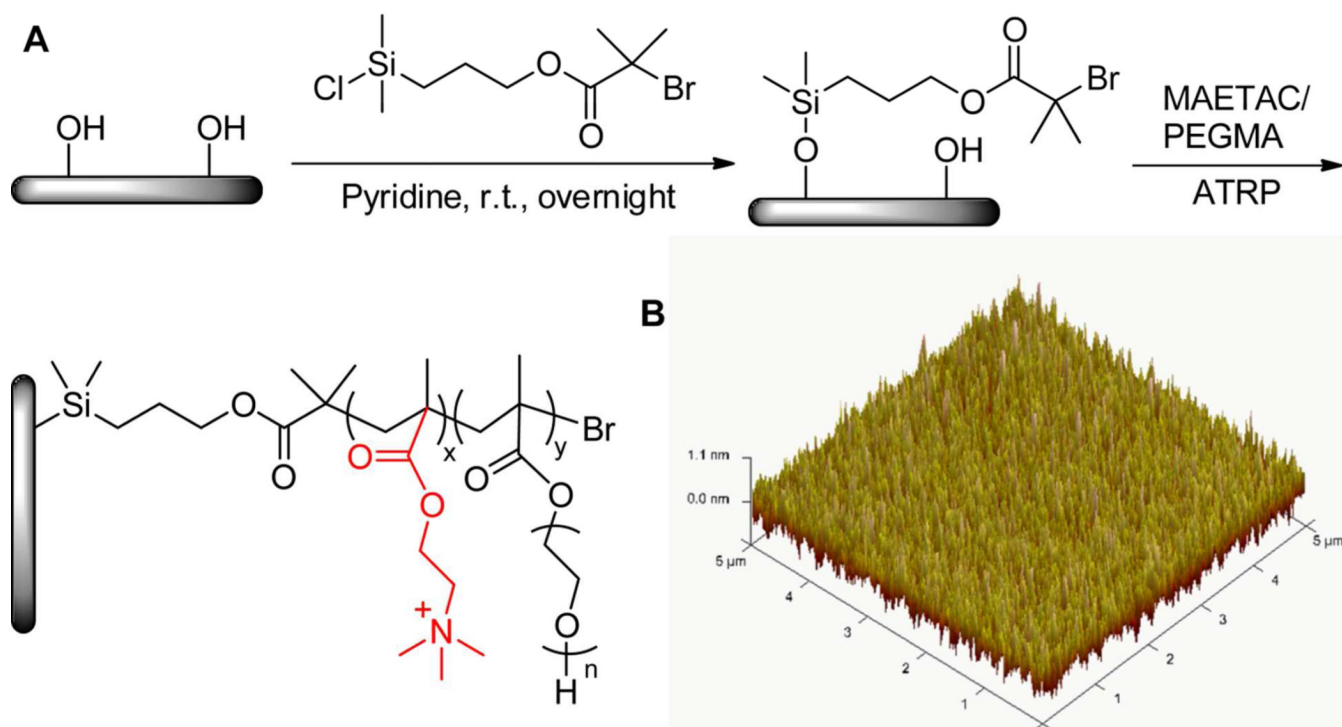


**Figure 1.**

A) Schematic representation of initiator attachment to silicon surface and polymerization of monomers using a surface-initiated ATRP approach. Chemical structure of tethered acetylcholine was also highlighted (red) in the resulting polymer brushes. B) AFM image of poly(PEGMA-*ran*-MAETAC) brushes on silicon substrate (  $5 \mu\text{m} \times 5 \mu\text{m}$ ,  $R_a = 0.25 \text{ nm}$ ).

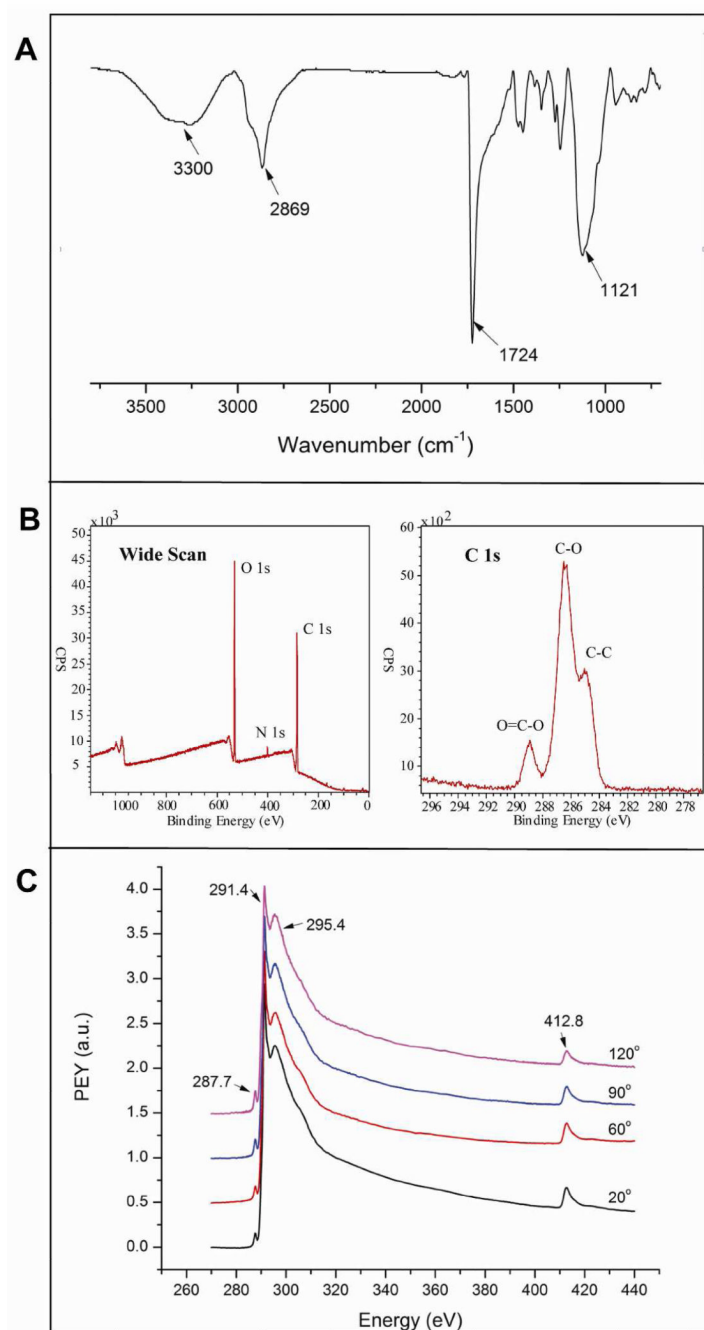


**Figure 2.** Characterization of poly(PEGMA-ran-MAETAC) brushes on silicon substrate. A) ATR-FTIR reflectance spectrum under nitrogen atmosphere. B) XPS wide scan (left) and C1s core level spectrum of the polymer brushes. C) NEXAFS spectra of brushes on silicon wafer at four different angles.

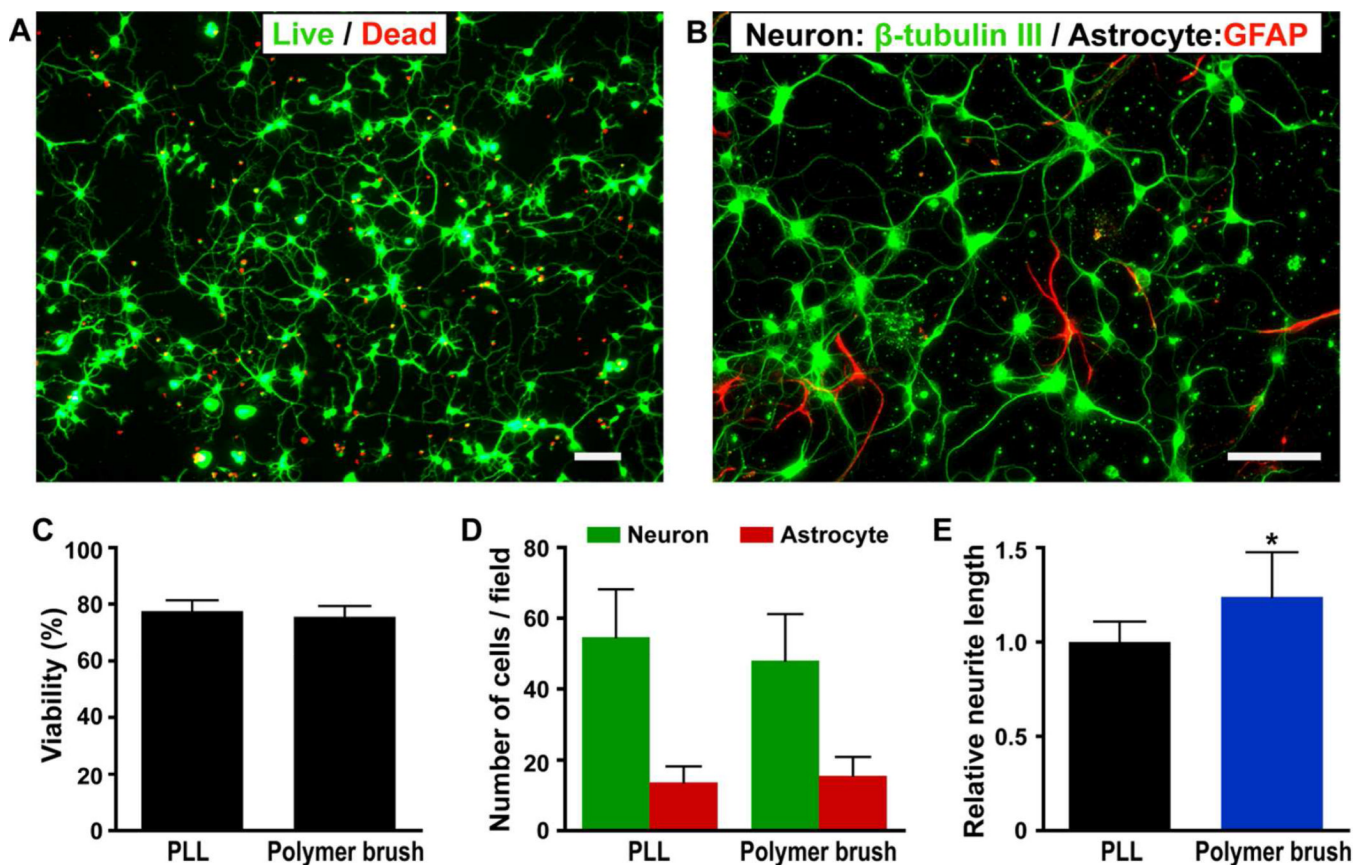


**Figure 3.**

Photographs of mouse hippocampal neuronal cells cultured on polymer brush modified silicon surfaces and data comparison with those on poly-L-lysine coated glass slides. A) LIVE/DEAD viability/cytotoxicity assay of hippocampal cells on polymer brushes (scale bar is 50  $\mu\text{m}$ ). Cells were cultured for three days and observed with fluorescent micrographs of live (calcein AM, green) and dead (ethidium homodimer-1, red). B) Immunocytochemistry demonstrates that neurons ( $\beta$ -III-tubulin-positive cells, green) outnumber astrocytes (GFAP-positive cells, red) on the surface. (Scale bar is 50  $\mu\text{m}$ ). C) Viability of cells on polymer brush is comparable to that of PLL coated glass slides. D) Similar number of neurons and astrocytes were observed on polymer brushes and the PLL control surfaces. E) Neurons on polymer brush surface exhibit longer neurites as compared to those on the PLL coated glass slides.

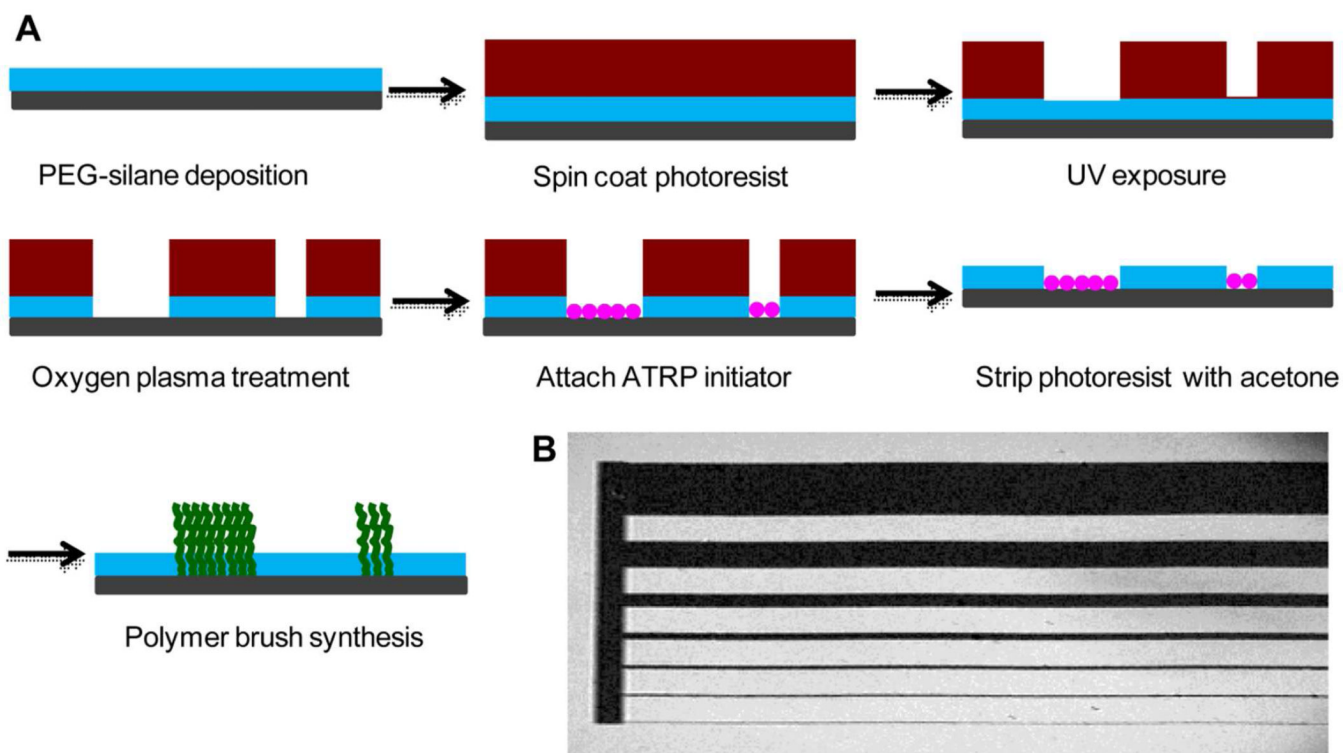


**Figure 4.** A) Surface modification steps used to create patterned polymer brushes *via* photolithographic techniques, and B) ellipsometry mapping photograph of patterned brushes on silicon wafer.

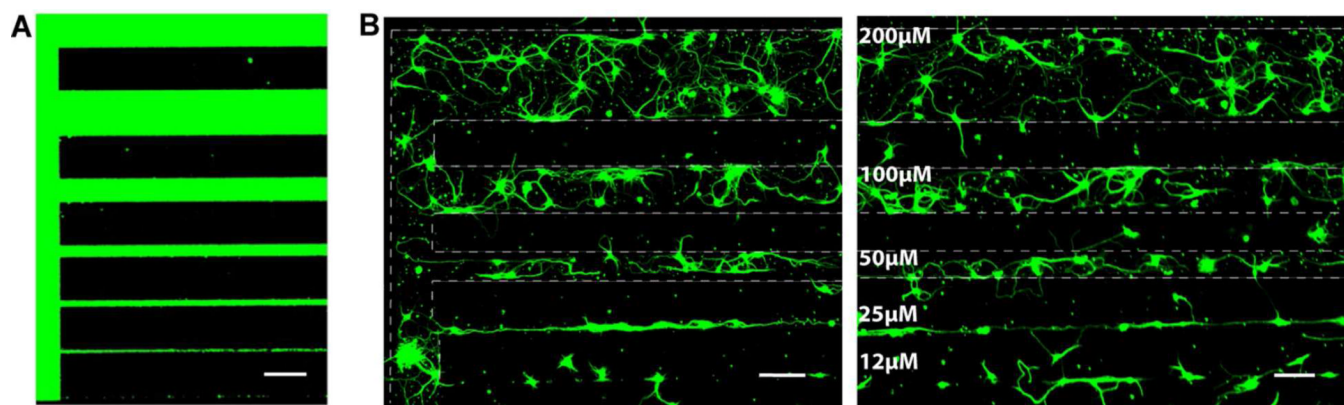


**Figure 5.** A) Patterned FTIC-BSA and B) patterned mouse hippocampal neuronal cells on the poly(PEGMA-ran-MAETAC) brush surfaces (scale bar is 100  $\mu\text{m}$ ). Dashed lines were added as visual guide for the patterned cells.